

Responsive Supramolecular Polymers Based on the Bis[alkynylplatinum(II)] Terpyridine Molecular Tweezer/Arene Recognition Motif**

Yu-Kui Tian, Yong-Gang Shi, Zhi-Shuai Yang, and Feng Wang*

Abstract: Supramolecular polymers are constructed based on the novel bis[alkynylplatinum(II)] terpyridine molecular tweezer/pyrene recognition motif. Successive addition of anthracene as the diene and cyano-functionalized dienophile triggers the reversible supramolecular polymerization process, thus advancing the concept of utilizing Diels–Alder chemistry to access stimuli-responsive materials in compartmentalized systems.

Supramolecular polymers are defined as polymeric arrays held together by reversible noncovalent interactions, and the fundamental recognition motifs exert considerable influence on their macroscopic properties.^[1] Macrocyclic hosts and their complementary guests, attributing to the high directional and inherent responsive properties for host–guest interactions, have been widely exploited for the construction of supramolecular polymers.^[2–5] However, these macrocyclic hosts are commonly symmetrical and rigid, thus not only resulting in poor solubility, but also suffering from problems such as tedious synthesis and low yield for the functionalization of the host. Additionally, guest species suitable for encapsulation into the macrocyclic hosts are rather limited. In this respect, acyclic receptors such as molecular tweezers, on account of their preorganized yet sufficient flexible properties, could sandwich a variety of guest moieties and overcome the limitations encountered by their macrocyclic counterparts.^[6] Up to now, little effort has been devoted to replacing macrocyclic hosts by the tweezer receptor,^[7] which expands the host–guest toolbox and represents a more versatile strategy for the fabrication of supramolecular polymeric assemblies.

Recently, Yam and co-workers described a novel molecular tweezer possessing two pincerlike alkynylplatinum(II) terpyridine units connected by rigid spacer.^[8] The predetermined distance of the two electron-deficient pincers facilitates recognition of a variety of electron-rich arenes through charge-transfer interactions. Inspired by these results, we

endeavored to construct well-organized supramolecular polymeric arrays based on such a tweezer/arene recognition motif. Specifically, we designed the molecular tweezer **1** having pendant hydroxy group, which efficiently tethers the complementary pyrene unit to afford the heteroditopic AB-type monomers **2–3** (Scheme 1). Enthalpically favorable tweezer/pyrene complexation guarantees the formation of the linear supramolecular polymers **4** in a head-to-tail fashion. The presence of flexible alkyl spacers on **2** and **3** is expected to decrease conformational entropy for the multiple tweezer/pyrene recognition processes.^[9]

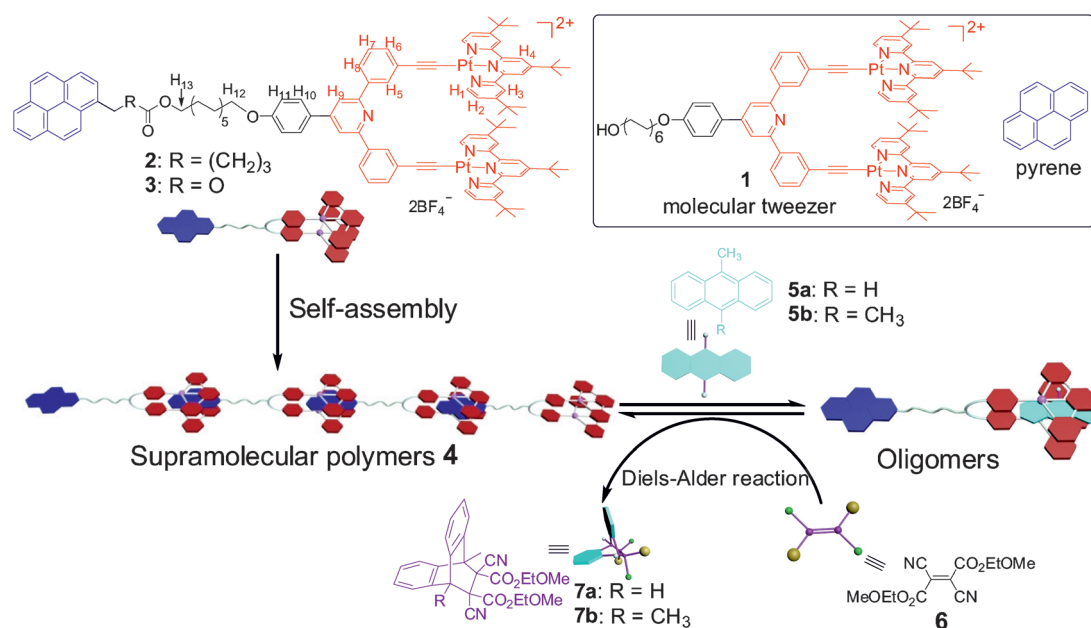
On this basis, we sought to impart stimuli-responsive properties to the resulting supramolecular polymers **4** by taking advantage of the unique tweezer/arene recognition behavior. To date, the switching elements in response to external stimuli are predominantly embedded in the supramolecular building blocks themselves.^[10] In contrast, employment of a second component as the stimuli-responsive auxiliary, which allows for the emergence of cascade signal transduction, has been far-less explored.^[11] It should be noted that such a protocol is advantageous for the achievement of programmed supramolecular systems having increasing complexity.^[12] Herein, the anthracene derivatives **5** (Scheme 1) were chosen as the auxiliaries, based on the following two considerations. First, in view of the planar and aromatic structural features, **5** could potentially enter the cavity of the molecular tweezer and thus serve as the chain stoppers to trigger the disassembly of the supramolecular polymers **4**. Second, **5** has been proven to undergo Diels–Alder reactions with the cyano-functionalized dienophile **6** to quantitatively afford the adducts **7**,^[13] which disrupts the planarity and aromaticity of the anthracene moieties and would thereby decomplex from the molecular tweezer unit. Consequently, it leads to the reformation of the supramolecular polymers **4** in compartmentalized systems. Therefore, we anticipate that with the elaborate manipulation of Diels–Alder chemistry, the supramolecular polymerization process, directed by tweezer/arene recognition, could be precisely regulated.

The synthetic routes towards the targeted compounds **1–3** are quite straightforward (see Schemes S1–S3 in the Supporting Information). The key step involves a diphenylammonium triflate (DPAT) catalyzed synthesis of the diphenylpyridine backbone (Scheme S1), thus representing a new and convenient method to access the tweezer structure having a pendant functional group. Subsequent condensation of **10** with pyrene derivatives, followed by copper(I)-catalyzed coupling with chloroplatinum(II) terpyridine, afforded the desired heteroditopic monomers **2** and **3** (Schemes S2–S3). The proposed structures of the synthetic compounds were verified by NMR

[*] T.-K. Tian, Y.-G. Shi, Z.-S. Yang, Dr. F. Wang
Key Laboratory of Soft Matter Chemistry, Department of Polymer Science and Engineering, University of Science and Technology of China, Hefei, Anhui 230026 (P. R. China)
E-mail: drfwang@ustc.edu.cn

[**] This work was supported by the National Natural Science Foundation of China (21274139, 91227119), the Fundamental Research Funds for the Central Universities (WK2060200012), and Anhui Provincial Natural Science Foundation (1208085QB22).

Supporting information for this article is available on the WWW under <http://dx.doi.org/10.1002/anie.201402192>.



Scheme 1. Schematic representation for the utilization of Diels–Alder chemistry to access responsive supramolecular polymers **4** derived from the monomers **2** and **3**. The bis[alkynyl]platinum(II) terpyridine molecular tweezer/pyrene recognition motif is shown in the frame.

spectroscopy and mass spectra (see Figures S1–S21 in the Supporting Information). The bulky *tert*-butyl groups on the molecular tweezer could significantly prevent self-association and thereby enhance solubility in chlorinated solvents.

Noncovalent complexation between the molecular tweezer **1** and pyrene was first clarified. For **1** itself, signal broadening phenomenon is observed for the aromatic protons in the ^1H NMR spectrum and is mainly ascribed to the irregular capture of one diphenylpyridine by another molecular tweezer unit (see Figure S13 in the Supporting Information). In contrast, upon addition of equimolar amounts of pyrene to **1**, the resulting ^1H NMR spectrum shows defined sharp signals, which definitely supports the preferential complexation between **1** and pyrene (see Figure S24f in the Supporting Information). Furthermore, the molar ratio plot, derived from ^1H NMR titration experiments, provides the explicit evidence for 1:1 binding stoichiometry between **1** and pyrene (see Figure S23 in the Supporting Information). Temperature-dependent ^1H NMR measurements for an equimolar solution of **1** and pyrene in $[\text{D}_2]$ tetrachloroethane were also performed (see Figure S24 in the Supporting Information). Briefly, both the terpyridine protons on **1** and the pyrene protons exhibit remarkable downfield shifts at elevated temperature, while no obvious changes occur for the diphenylpyridine protons. Hence, it validates that intermolecular charge-transfer interactions between the platinum(II) terpyridine and pyrene units are the intrinsic driving forces for molecular tweezer/pyrene complexation.

Alkynylplatinum(II) terpyridine units possess interesting optical properties, which makes it easier for us to evaluate the tweezer/guest binding affinity using spectroscopic techniques.^[8,14] For **1**, MLCT (metal-to-ligand charge transfer) and LLCT (ligand-to-ligand charge transfer) bands are located predominately between $\lambda = 400$ and 500 nm in UV/

Vis spectrum (Figure 1a, inset), meanwhile the maximum emission signal appears at $\lambda = 584$ nm (Figure 1b, inset). Progressive addition of 1-pyrenemethanol to **1** leads to a gradual decrease of the intensity for the MLCT/LLCT absorption bands (Figure 1a). Treatment of the collected

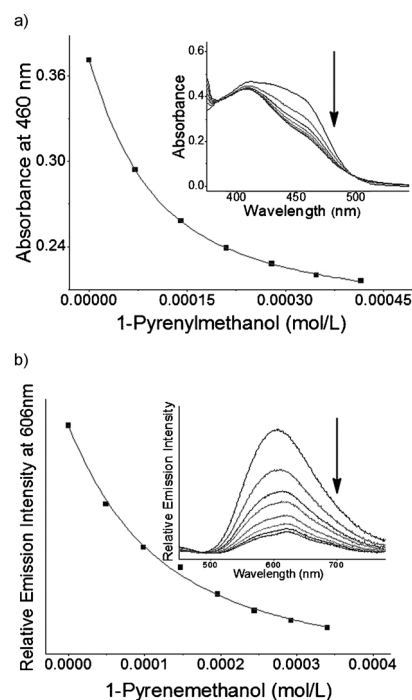


Figure 1. The intensity changes of a) absorbance at $\lambda = 460$ nm and b) emission intensity at $\lambda = 606$ nm upon addition of 1-pyrenemethanol. The solid line was obtained from the nonlinear curve-fitting. Insets: arrows show a) UV/Vis absorption and b) emission spectral changes of **1** (5.00×10^{-5} M) upon addition of 1-pyrenemethanol.

absorbance data at $\lambda = 460$ nm with a nonlinear curve-fitting equation [see Eq.(S1) in the Supporting Information] afforded the corresponding association constant $K_a = (1.43 \pm 0.02) \times 10^4 \text{ M}^{-1}$ for **1**/1-pyrenemethanol. A similar result [$K_a = (1.11 \pm 0.10) \times 10^4 \text{ M}^{-1}$] was also acquired based on the titration curve obtained from fluorescence data (Figure 1b). When unsubstituted pyrene acts as the guest, the association constants calculated from UV/Vis and fluorescent measurements are $(2.27 \pm 0.05) \times 10^3 \text{ M}^{-1}$ and $(4.17 \pm 0.05) \times 10^3 \text{ M}^{-1}$, respectively (see Figure S25 in the Supporting Information). All of the titration experiments confirm the strong tweezer/pyrene complexation behavior, which lays the foundation for the construction of the supramolecular polymers **4**.^[15]

We then turned to examining the supramolecular polymerization behavior for the two heteroditopic monomers **2** and **3**. ^1H NMR measurements show that the tweezer/pyrene complex is susceptible to temperature variation (Figure 2). At

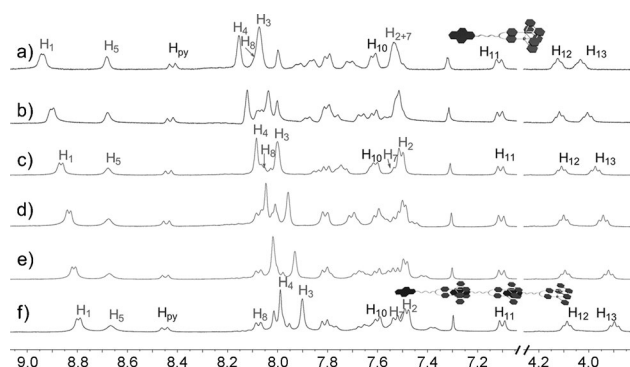


Figure 2. Partial ^1H NMR spectra (400 MHz, $\text{C}_2\text{D}_2\text{Cl}_4$) of **2** (20.0 mM) at different temperatures: a) 363; b) 348; c) 333; d) 318; e) 308; f) 298 K. H_{py} denotes the protons on pyrene unit.

high temperature, the ^1H NMR spectrum of **2** exhibits well-defined sharp signals (Figure 2a), thus indicating the dominance of monomeric species. When the solution was cooled down from 363 K to 298 K, H_{py} and H_{13} , which neighbor the pyrene unit, exhibit slight downfield and upfield shifts, respectively. Meanwhile, the pincer terpyridine protons $\text{H}_{1,3,4}$ appear in the upfield region ($\Delta\delta = -0.15$, -0.17 and -0.17 ppm for H_1 , H_3 , and H_4 , respectively; Figure 2). The apparent chemical shift changes demonstrate the temperature-dependent encapsulation of pyrene into the cavity of the molecular tweezer unit.

Concentration-dependent ^1H NMR spectra of **2** were also recorded at monomer concentrations between 0.44 and 31.1 mM (see Figure S29 in the Supporting Information). Only one set of aromatic signals is present in the ^1H NMR spectra, thus revealing the involvement of fast-exchanging noncovalent interactions on the NMR time scale. At high monomer concentration, significant upfield shifts are observed for the aromatic protons, along with the broadening of all signals. A similar trend is also visualized for **3** (see Figure S30 in Supporting Information), thus indicating that both heteroditopic monomers are prone to aggregating into high-molecular-weight assemblies with reduced mobility.

Furthermore, sizes of the resulting assemblies were also probed by two-dimensional diffusion-ordered NMR (DOSY) spectra (see Figure S31 in the Supporting Information). As the concentration of **2** increases from 5.00 mM to 80.0 mM, the measured diffusion coefficients decrease dramatically from 8.58×10^{-10} to $1.48 \times 10^{-10} \text{ m}^2 \text{ s}^{-1}$. A similar tendency is observed for the monomer **3**, for which the diffusion coefficients decline from 6.84×10^{-10} to $1.01 \times 10^{-10} \text{ m}^2 \text{ s}^{-1}$ under the same conditions. Hence, it is obvious that both temperature and monomer concentration exert crucial impacts on the formation of **4**.

Viscosity experiments were performed to gain further insight into the supramolecular polymerization process. For the two heteroditopic monomers **2** and **3**, both measurements show distinct slope changes in the double logarithmic plots of specific viscosity versus concentration (Figure 3a). In the low concentration range, the slopes exhibit the values of 1.29 for **2** and 1.35 for **3**, thus indicating the dominance of cyclic oligomers with constant size. Remarkably, when the concen-

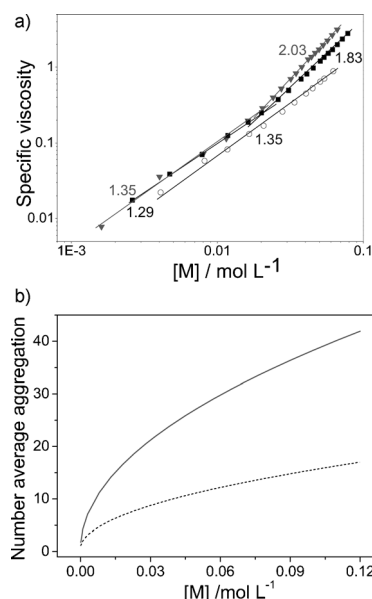


Figure 3. a) Specific viscosity (chloroform, 298 K) of **1** (\circ), **2** (\blacksquare), and **3** (\blacktriangledown) versus the monomer concentration. b) Estimated number average degree of polymerization (N) of **2** (solid line) and **3** (dash line) as a function of monomer concentration.

tration exceeds the critical polymerization concentration value (around 20 mM for both monomers), the curves of **2** and **3** approach the slopes of 1.83 and 2.03, respectively. Such results denote the favorable transitions from cyclic species to linear chains at high monomer concentration, and is consistent with a ring-chain transition mechanism.^[1a] In contrast, no obvious slope change occurs for the monotopic molecular tweezer **1** (slope = 1.35). Considering that **1–3** possess the same π -conjugated units [alkynylplatinum(II) terpyridine groups], meanwhile the pyrene moiety in both **2** and **3** cannot stack on each other because it sits in the cavity of the molecular tweezer, chain extension of the heteroditopic monomers **2–3** at high monomer concentration can be mainly ascribed to the effect of tweezer/pyrene complexation rather than π – π stacking interactions. In addition, fibers could

be drawn from a concentrated solution of **2**, characteristic for the entanglement of linear supramolecular polymers forming connected macrosized aggregates (see Figure S33 in the Supporting Information).

It is noteworthy that **3** tends to form relatively large polymeric assemblies compared to those of **2**, as depicted by the higher slope (1.83 for **2** versus 2.03 for **3** for viscosity measurements) and lower diffusion coefficient values (1.48×10^{-10} for **2** versus $1.01 \times 10^{-10} \text{ m}^2 \text{ s}^{-1}$ for **3** for DOSY measurements). The isodesmic model was then chosen to theoretically calculate the average degree of polymerization, N , for the resulting supramolecular polymers (Figure 3b and the Equation S3 in the Supporting Information). Briefly, when the monomer concentration of **3** approaches 70 mmol L^{-1} , N is approximately 32 (total molar mass is $6.97 \times 10^4 \text{ g mol}^{-1}$), whilst for **2** N is calculated to be 13 under the same conditions.^[1a,15,16] Hence, it suggests that different spacers on the heteroditopic monomers influence the charge density of the neighboring pyrene unit, thus leading to the stronger tweezer/guest complexation in the case of **3**.

Next, stimuli-responsive properties of the resulting supramolecular polymers **4** were investigated by taking advantage of anthracene derivatives **5** as the chain-stopper moieties. The recognition behavior between **5** and the monotopic receptor **1** was first tested, for which the K_a values were determined to be $(3.33 \pm 0.11) \times 10^3 \text{ M}^{-1}$ and $(1.10 \pm 0.02) \times 10^3 \text{ M}^{-1}$ for 9-methylanthracene (**5a**) and 9,10-dimethylanthracene (**5b**), respectively (see Figure S26 in the Supporting Information). The decreased binding affinity for **5b** implies that two methyl substituents on the anthracene impart steric hindrance for tweezer/guest association. Subsequently, the influence of anthracene additives on the depolymerization of the heteroditopic monomer **2** was monitored by ^1H NMR titration experiments (Figure 4a–f). Upon progressive addition of **5a** to **2**, the pyrene unit is gradually converted to the uncomplexed state, as manifested by the apparent upfield shift for the proton H_{py} (Figure 4a–f) and downfield shift for the proton H_{13} (see Figure S34 in the Supporting Information), which is in agreement with the tendency observed in Figure 2. Meanwhile, protons $\text{H}_{1,3,4}$ on the terpyridine unit shift upfield considerably (Figure 4a–f). Such phenomena demonstrate that **5a** could act as the competitive guest to complex with the tweezer unit, thus giving rise to the stoichiometry imbalance between the molecular tweezer and pyrene moieties, and thereby leading to the disruption of supramolecular polymers **4**. The conclusion is further supported by the theoretical calculations (see Figure S41 in the Supporting Information). Particularly, when 1 equivalent of **5a** is added to **2** at 70.0 mM , the estimated degree of polymerization for the resulting supramolecular polymers decreases significantly from approximately 13 to 2. When **2** is replaced by **3**, the calculated value varies from approximately 32 to 3. Meanwhile, both NMR titration experiments (see Figure S36 in the Supporting Information) and theoretical calculations (see Figure S41 in the Supporting Information) reveal that the degree of polymerization value changes to a lesser extent with the addition of **5b**, and is consistent with its weaker binding affinity towards the tweezer receptor when compared with that of **5a**.

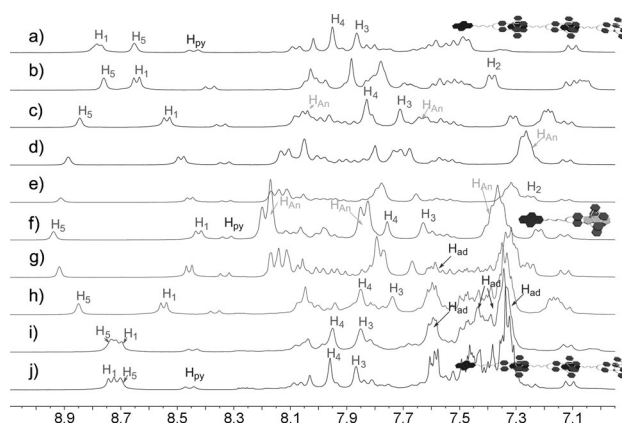


Figure 4. Partial ^1H NMR spectra (300 MHz, 298 K) of **2** (20.0 mM) upon successive additions of **5a** and **6**: a) 0 equiv; b) 0.5 equiv; c) 1.5 equiv; d) 2.6 equiv; e) 3.7 equiv; f) 5.2 equiv of **5a**; g) 5.2 equiv of **5a** and 1.4 equiv of **6**; h) 5.2 equiv of **5a** and 3.6 equiv of **6**; i) 5.2 equiv of **5a** and 5.1 equiv of **6**; j) 5.2 equiv of **5a** and 8.0 equiv of **6**. H_{py} , H_{An} , and H_{Ad} denote the protons on pyrene unit, **5a**, and **7a**, respectively.

We further tested the feasibility of reforming the supramolecular polymers **4**, by making use of the facile room-temperature Diels–Alder reaction between **5** and **6**. It raises the question as to whether the specific reaction could be smoothly proceed in the presence of another arene moiety. To address the issue, we first investigated the model system comprising equimolar mixtures of pyrene, **5**, and **6**, and the results clearly support the quantitative conversion of the latter two compounds into the cycloaddition adduct without the participation of pyrene unit (see Figures S38 and S39 in the Supporting Information). On this basis, **6** was titrated into the above mixtures of **2** and **5a** (Figure 4f), thus resulting in the progressive signal conversion to the initial polymeric state (Figure 4g–j). The original signals arising from **4** were restored upon the addition of excess amounts of **6** (Figure 4i), thus demonstrating that the Diels–Alder reaction is efficient within the multicomponent system and leads to the reassembly of supramolecular polymeric assemblies.

The interplay between the Diels–Alder reaction and reversible supramolecular polymerization in the complex systems could be monitored by DOSY experiments (Figure 5). Practically, when 1.0 equivalent of **5a** was added into monomer **2** at 70 mM (linear polymeric species play a prominent role at this concentration), the diffusion coefficient values increase from 2.45×10^{-10} to $8.20 \times 10^{-10} \text{ m}^2 \text{ s}^{-1}$. The significant size shrinking mainly correlates to the disassembly of **4**. Further addition of 3.5 equivalents of **6** induces the reassembly process, observed from the transition of the coefficient value back to $1.84 \times 10^{-10} \text{ m}^2 \text{ s}^{-1}$.^[17] Hence, based on the ^1H NMR titration and DOSY measurements, it is evident that the supramolecular polymers **4** are highly adaptive and capable of undergoing reversible transitions triggered by Diels–Alder chemistry.

In summary, we have successfully constructed linear supramolecular polymers based on the novel bis[alkynylplatinum(II)] terpyridine molecular tweezer/pyrene recognition motif. The head-to-tail supramolecular polymerization pro-

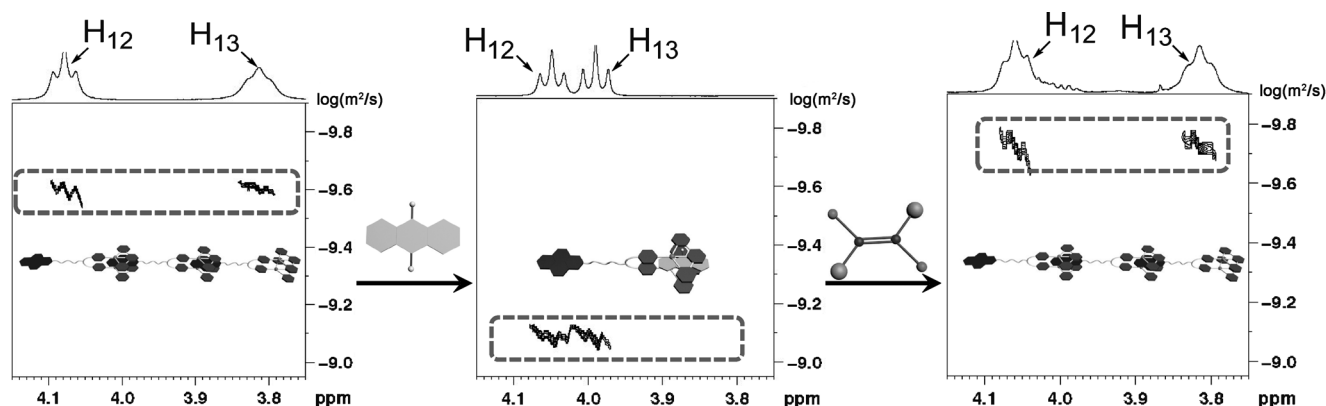


Figure 5. DOSY spectra (400 MHz, CDCl_3 , 298 K) of **2** (70 mM) with successive additions of 1.0 equiv of **5a** and 3.5 equiv of **6**.

cess conforms to a ring-chain equilibrium mechanism, requiring judicious choice of the relevant parameters such as monomer structures, concentration, and temperature to achieve favorable linear chain extension. Moreover, successive addition of the anthracene derivatives **5** and bis(2-methoxyethyl) dicyanofumarate **6** to the heteroditopic monomers triggers a reversible disassembly and reassembly processes, respectively, and advances the concept of utilizing Diels–Alder chemistry to achieve stimuli-responsive materials. The novel supramolecular polymer systems, which are regulated in a facile and controlled manner, motivate us to explore their potential applications such as sensing and tunable optoelectronic devices in the future.

Received: February 7, 2014

Revised: March 31, 2014

Published online: May 8, 2014

Keywords: cycloaddition · noncovalent interactions · platinum · polymers · supramolecular chemistry

- [1] a) T. F. A. De Greef, M. M. J. Smulders, M. Wolffs, A. P. H. J. Schenning, R. P. Sijbesma, E. W. Meijer, *Chem. Rev.* **2009**, *109*, 5687–5754; b) T. Aida, E. W. Meijer, S. I. Stupp, *Science* **2012**, *335*, 813–817; c) T. Haino, *Polym. J.* **2013**, *45*, 363–383.
- [2] a) S. Dong, B. Zheng, D. Xu, X. Yan, M. Zhang, F. Huang, *Adv. Mater.* **2012**, *24*, 3191–3195; b) M. Zhang, D. Xu, X. Yan, J. Chen, S. Dong, B. Zheng, F. Huang, *Angew. Chem.* **2012**, *124*, 7117–7121; *Angew. Chem. Int. Ed.* **2012**, *51*, 7011–7015; c) X. Yan, D. Xu, X. Chi, J. Chen, S. Dong, X. Ding, Y. Yu, F. Huang, *Adv. Mater.* **2013**, *25*, 362–369; d) X. Ji, Y. Yao, J. Li, X. Yan, F. Huang, *J. Am. Chem. Soc.* **2011**, *133*, 74–77; e) X. Ji, S. Dong, P. Wei, D. Xia, F. Huang, *Adv. Mater.* **2013**, *25*, 5725–5729.
- [3] M. Nakahata, Y. Takashima, H. Yamaguchi, A. Harada, *Nat. Commun.* **2011**, *2*, 511.
- [4] a) R. M. Yebeutou, F. Tancini, N. Demitri, S. Geremia, R. Mendichi, E. Dalcanele, *Angew. Chem.* **2008**, *120*, 4580–4584; *Angew. Chem. Int. Ed.* **2008**, *47*, 4504–4508; b) R. Sun, C. Xue, X. Ma, M. Gao, H. Tian, Q. Li, *J. Am. Chem. Soc.* **2013**, *135*, 5990–5993.
- [5] a) Y. Liu, Y. Yu, J. Gao, Z. Wang, X. Zhang, *Angew. Chem.* **2010**, *122*, 6726–6729; *Angew. Chem. Int. Ed.* **2010**, *49*, 6576–6579; b) E. A. Appel, X. J. Loh, S. T. Jones, F. Biedermann, C. A. Dreiss, O. A. Scherman, *J. Am. Chem. Soc.* **2012**, *134*, 11767–11773.
- [6] a) M. Hardouin-Lerouge, P. Hudhomme, M. Salle, *Chem. Soc. Rev.* **2011**, *40*, 30–43; b) D. Ma, G. Hettiarachchi, D. Nguyen, B. Zhang, J. B. Wittenberg, P. Y. Zavalij, V. Briken, L. Isaacs, *Nat. Chem.* **2012**, *4*, 503–510; c) T. Haino, A. Watanabe, T. Hirao, T. Ikeda, *Angew. Chem.* **2012**, *124*, 1502–1505; *Angew. Chem. Int. Ed.* **2012**, *51*, 1473–1476.
- [7] a) G. Fernández, E. M. Perez, L. Sanchez, N. Martin, *Angew. Chem.* **2008**, *120*, 1110–1113; *Angew. Chem. Int. Ed.* **2008**, *47*, 1094–1097; b) S. Burattini, B. W. Greenland, W. Hayes, M. E. Mackay, S. J. Rowan, H. M. Colquhoun, *Chem. Mater.* **2011**, *23*, 6–8; c) J. S. Park, K. Y. Yoon, D. S. Kim, V. M. Lynch, C. W. Bielawski, K. P. Johnston, J. L. Sessler, *Proc. Natl. Acad. Sci. USA* **2011**, *108*, 20913–20917; d) D. S. Kim, V. M. Lynch, J. S. Park, J. L. Sessler, *J. Am. Chem. Soc.* **2013**, *135*, 14889–14894.
- [8] a) Y. Tanaka, K. M.-C. Wong, V. W.-W. Yam, *Chem. Sci.* **2012**, *3*, 1185–1191; b) Y. Tanaka, K. M.-C. Wong, V. W.-W. Yam, *Chem. Eur. J.* **2013**, *19*, 390–399; c) Y. Tanaka, K. M.-C. Wong, V. W.-W. Yam, *Angew. Chem.* **2013**, *125*, 14367–14370; *Angew. Chem. Int. Ed.* **2013**, *52*, 14117–14120.
- [9] H. W. Gibson, N. Yamaguchi, J. W. Jones, *J. Am. Chem. Soc.* **2003**, *125*, 3522–3533.
- [10] a) B. Rybtchinski, *ACS Nano* **2011**, *5*, 6791–6818; b) X. Yan, F. Wang, B. Zheng, F. Huang, *Chem. Soc. Rev.* **2012**, *41*, 6042–6065.
- [11] a) F. Helmich, C. C. Lee, A. P. H. J. Schenning, E. W. Meijer, *J. Am. Chem. Soc.* **2010**, *132*, 16753–16755; b) T. Hirose, F. Helmich, E. W. Meijer, *Angew. Chem.* **2013**, *125*, 322–327; *Angew. Chem. Int. Ed.* **2013**, *52*, 304–309.
- [12] J.-M. Lehn, *Proc. Natl. Acad. Sci. USA* **2002**, *99*, 4763–4768.
- [13] P. Reutenauer, P. J. Boul, J.-M. Lehn, *Eur. J. Org. Chem.* **2009**, 1691–1697.
- [14] a) K. M.-C. Wong, V. W.-W. Yam, *Acc. Chem. Res.* **2011**, *44*, 424–434; b) S. Y.-L. Leung, A. Y.-Y. Tam, C.-H. Tao, H. S. Chow, V. W.-W. Yam, *J. Am. Chem. Soc.* **2012**, *134*, 1047–1056.
- [15] L. Brunsveld, B. J. B. Folmer, E. W. Meijer, R. P. Sijbesma, *Chem. Rev.* **2001**, *101*, 4071–4098.
- [16] It should be noted that N calculated in this way represents the maximum values which in practice will be reduced by the formation of cyclic species. F. Huang, D. S. Nagvekar, X. Zhou, H. W. Gibson, *Macromolecules* **2007**, *40*, 3561–3567.
- [17] The slight fluctuation of the coefficient values before and after the switching cycle (2.45×10^{-10} and $1.84 \times 10^{-10} \text{ m}^2 \text{ s}^{-1}$, respectively) could probably be ascribed to the two successive Diels–Alder additives, which alters the viscosity for the whole solution. S. Pappalardo, V. Villari, S. Slovak, Y. Cohen, G. Gattuso, A. Notti, A. Pappalardo, I. Pisagatti, M. F. Parisi, *Chem. Eur. J.* **2007**, *13*, 8164–8173.